Paper

# INFLUENCE OF NEUTRON SOURCES AND $^{10}$B CONCENTRATION ON BORON NEUTRON CAPTURE THERAPY FOR SHALLOW AND DEEPER NON-SMALL CELL LUNG CANCER

Haiyan Yu,* Xiaobin Tang,*† Diyun Shu,* Yuanhao Liu,* Changran Geng,*‡ Chunhui Gong,* Shuang Hang,* and Da Chen*†

*Abstract*—**Boron Neutron Capture Therapy (BNCT) is a radiotherapy that combines biological targeting and high Linear Energy Transfer (LET). It is considered a potential therapeutic approach for non-small cell lung cancer (NSCLC). It could avoid the inaccurate treatment caused by the lung motion during radiotherapy, because the dose deposition mainly depends on the boron localization and neutron source. Thus, $^{10}$B concentration and neutron sources are both principal factors of BNCT, and they play significant roles in the curative effect of BNCT for different cases. The purpose was to explore the feasibility of BNCT treatment for NSCLC with either of two neutron sources (the epithermal reactor at the Massachusetts Institute of Technology named "MIT source" and the accelerator neutron source designed in Argentina named "MEC source") and various boron concentrations. Shallow and deeper lung tumors were defined in the Chinese hybrid radiation phantom, and the Monte Carlo method was used to calculate the dose to tumors and healthy organs. The MEC source was more appropriate to treat the shallow tumor (depth of 6 cm) with a shorter treatment time. However, the MIT source was more suitable for deep lung tumor (depth of 9 cm) treatment, as the MEC source is more likely to exceed the skin dose limit. Thus, a neutron source consisting of more fast neutrons is not necessarily suitable for deep treatment of lung tumors. Theoretical distribution of $^{10}$B in tumors and organs at risk (especially skin) was obtained to meet the treatable requirement of BNCT, which may provide the references to identify the feasibility of BNCT for the treatment of lung cancer using these two neutron sources in future clinical applications.**
**Health Phys. 112(3):258–265; 2017**

**Key words: cancer; Monte Carlo; radiation therapy; radiobiology**

## INTRODUCTION

Local non-small cell lung cancer (NSCLC), a common cause of cancer deaths worldwide, presents with limited therapeutic options because of tumor locations, which are mostly near the trachea. Cancer cells in this region require timely treatment since they may have diffused into the right lung but not to the whole body. Scholars have proposed boron neutron capture therapy (BNCT) for the treatment of NSCLC (Farias et al. 2014). BNCT combines biological targeting and high linear energy transfer (LET) radiation. As the exploited reaction $^{10}$B (n, alpha) $^{7}$Li is the neutron capture in $^{10}$B, which has a cross section of 3,837 b at thermal energies, the neutron capture gives rise to high LET radiation, generating an alpha particle and a $^{7}$Li nucleus with ranges in tissues comparable to a cell diameter. The energy deposition is spatially confined in the cells where neutrons are captured. Therefore, dose delivery in BNCT is selective at the cellular level. This therapy can avoid the inaccurate treatment caused by the motion of cancerous lung tissues during radiotherapy, as the major effect depends on boron localization. Moreover, the treatment may be delivered in a single-fraction through BNCT with less time and cost.

Clinical studies on BNCT indicate that the neutron source and distribution of boron concentration are key factors affecting the curative effect of this therapy (Sutlief 2015). The energy spectrum of the neutron sources plays an important role in the dose deposition (Sakurai and Ono 2007) in cancer patients. Dose delivery to healthy organs increases with increasing boron concentration in healthy tissues, and this phenomenon leads to increased cancer risk (Ryynanen et al. 2000). At present, the feasibility of applying BNCT to local lung cancer has been explored to ensure the efficacy and safety of this treatment (Matsumoto 2007; Krstic et al. 2014). Nevertheless, an in-depth study on the relationship of the curative effect of the neutron source and the distribution of boron concentration has not been conducted. Moreover, researchers used idealized phantoms [for instance, the ORNL phantom (Krstic et al. 2014)],

*Department of Nuclear Science and Engineering, Nanjing University of Aeronautics and Astronautics, 29 Yudao Street, 210016 Nanjing, China; †Collaborative Innovation Center of Radiation Medicine of Jiangsu Higher Education Institutions, 29 Yudao Street, 210016 Nanjing, China; ‡Department of Radiation Oncology, Massachusetts General Hospital, Boston, MA 02114.

For correspondence contact: Xiaobin Tang, Nanjing University of Aeronautics and Astronautics, Nanjing, China, or email at **tangxiaobin@nuaa.edu.cn**.

(*Manuscript accepted* 6 *September* 2016)
0017-9078/17/0


DOI: 10.1097/HP.0000000000000601

which exhibit morphological differences from actual human tissues and organs.

This study aims to determine theoretical boron-10 distribution under different neutron source irradiations in BNCT for local lung cancer treatment. Dose rates and components for cancerous lung tissues and healthy organs were calculated based on the third generation of the male Chinese hybrid radiation phantom (CHRP-Male) (Geng et al. 2014) by using the Monte Carlo method under various boron distributions and neutron sources.

## MATERIALS AND METHODS

### CHRP-Male phantom implementation

The CHRP-Male 30 phantom, representing a Chinese hybrid radiation phantom of a 30-y-old male (Fig. 1a), was used in this study for the Monte Carlo dose calculations. The phantom was built using Rhinoceros 5.0 (Guitton et al. 2013), and voxelizer series tools were employed to transform the phantom into a voxel-based model. Considering the geometry construction precision and the calculation speed in the Monte Carlo code used in this study, the phantom was voxelized with a resolution of $0.4 \times 0.4 \times 0.4$ cm$^3$. Tissue or organ compositions were from the data in ICRU 46 and ICRP 89 (ICRU 1992; ICRP 2002). Details of the construction procedure for the phantom geometry and materials have been described in a previous publication (Geng et al. 2014). Two cases were established: Case 1, shallow tumor (depth of 6 cm), and Case 2, deeper tumor (depth of 9 cm) models (Fig. 1b). The shape and size of tumors in the above two cases were both the same (volume: $7 \times 4 \times 3$ cm$^3$), so the cancerous lungs were divided into healthy lungs (grey) and the gross tumor volume (GTV) (black).

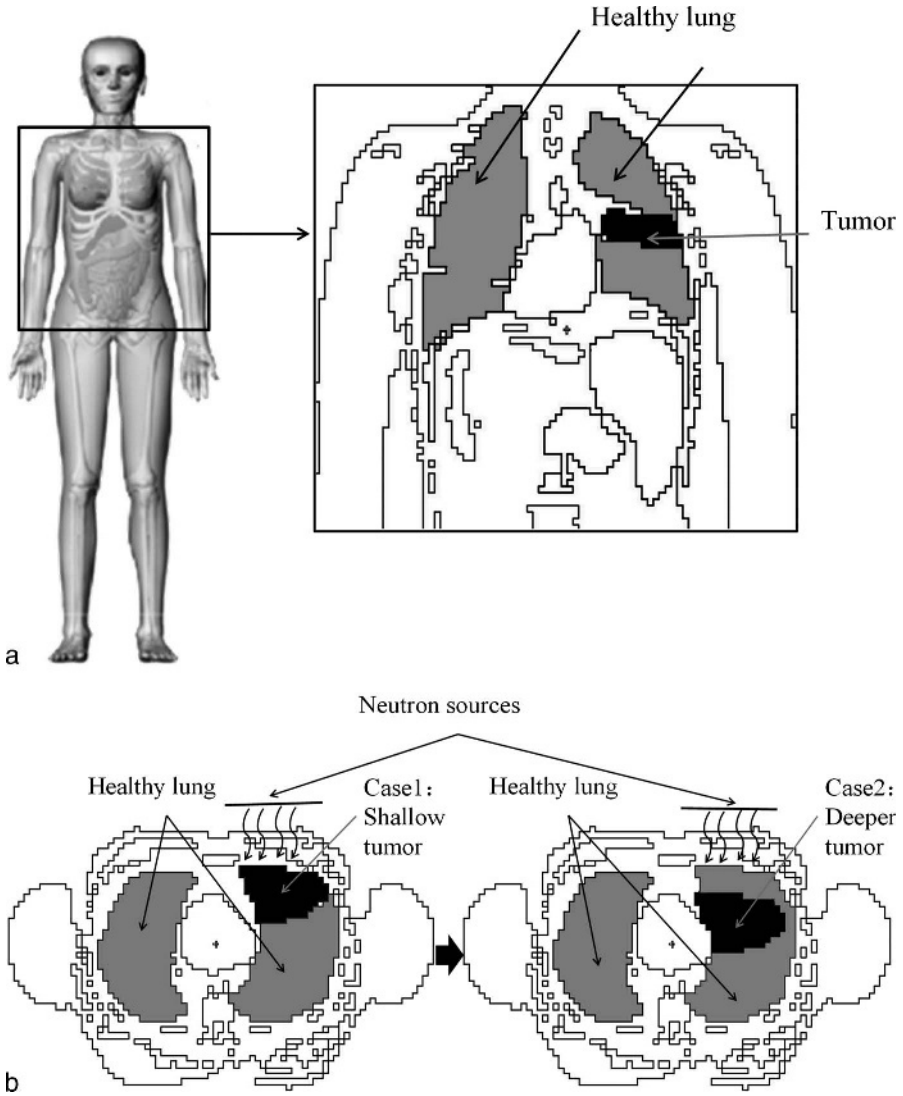


**Fig. 1.** The CHRP-Male phantom coded into MCNP5 and the emergent particles of the neutron source: (a) The longitudinal section of the CHRP-Male phantom; (b) the location of the case 1-shallow, and case 2-deeper tumor and neutron sources.

**Boron distribution models**

As the distribution of boron in tissues differs among various patients, the boron-10 concentration in cancerous lung tissues is between 25 ppm and 65 ppm (Coderre and Morris 1999). Meanwhile, boron-10 concentration in skin is between 6 ppm and 18 ppm (Table 1), and the ratios of boron in other organs at risk (OARs) to that in skin are considered as 1:1.5 (Mirzaei et al. 2014).

**Neutron sources**

Two realistic neutron spectra from existing or projected BNCT facilities were selected from the literature and evaluated. The first, named MIT-SPECT (abbreviated as MIT), is based on the published energy spectrum of the MIT-II epithermal reactor beam developed for BNCT (Riley et al. 2008). The second, named CNEA-MEC (abbreviated as MEC), is based on the energy spectrum published by Capoulat et al. (2014) for an accelerator-based epithermal neutron beam designed in Argentina for the treatment of deep-seated GBM tumors through BNCT. The spectra of these neutron beams are presented in Fig. 2. Source particles were sampled uniformly in a plane, and their particle direction was set mono-directionally, normal to that plane. Simulations of the beams were conducted by normalizing the corresponding thermal neutron flux peaks of the beams in water to $10^9$ n cm$^{-2}$ s$^{-1}$. Particle transport was performed without explicitly considering the unavoidable gamma contamination of the beam, and the dose induced by unavoidable gamma (contribution of radiation components) to the total dose was considered as equivalent to 50% of induced gamma dose due to the neutron reactions with $^1$H and $^{10}$B (Farias et al. 2014) in tissues.

The diameter of the source was 20 cm to encompass the tumor volume completely, and the neutron source emitted from the front of the tumor and the Source Skin Distance (SSD) was 3 cm (Fig. 1b). When the boron-10 concentration in tumor/skin was 65/18 ppm, the fast neutron dose on the surface induced by the MEC spectrum was higher than that irradiated by the MIT sources, and dose rates to areas of shallow and deeper tumor irradiated by the MEC was also higher than that induced by the MIT source (Fig. 3).

**Dose evaluations**

The dose of BNCT includes boron dose ($D_B$), thermal and fast neutron doses ($D_{th}$ and $D_f$), and gamma dose ($D_\gamma$). The dose stems from the interaction of thermal neutrons with $^{10}$B atoms in tissue through the $^{10}$B (n, alpha) $^7$Li reaction called $D_B$. The dose arises primarily from the

**Table 1.** The boron concentration in cancerous lung tissues and skin varied from 25–65 ppm and 6–18 ppm, respectively.

| | | | | | | | | | |
|---|---|---|---|---|---|---|---|---|---|
| Tumor (ppm) | 65 | 60 | 55 | 50 | 45 | 40 | 35 | 30 | 25 |
| Skin (ppm) | 18 | 16 | 14 | 12 | 10 | 9 | 8 | 7 | 6 |

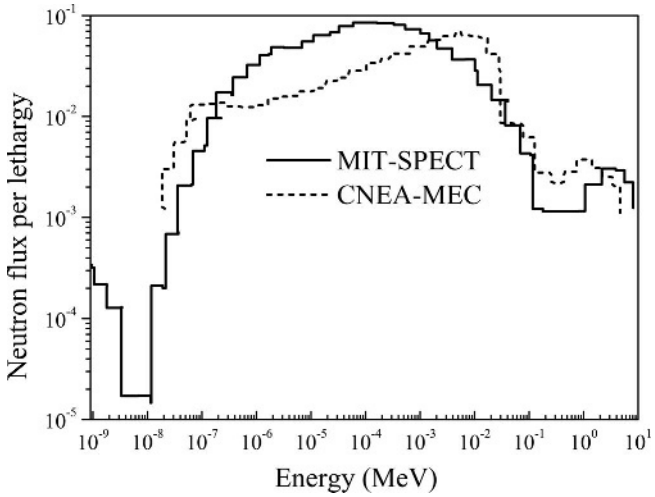


**Fig. 2.** Relative neutron flux per unit of lethargy as a function of energy for the MIT-SPECT beam based on the epithermal reactor and the CNEA-MEC beam based on the accelerator neutron source.

$^{14}$N (n, p) $^{14}$C thermal neutron capture reaction called $D_{th}$. Fast neutrons with energies above 10 keV deliver the dose through elastic collisions with hydrogen nuclei in tissue via the $^1$H (n, $n_0$)$^1$H reaction, called $D_f$. The dose component is related to photons that can be generated from unavoidable gamma contamination of the beam and induced gamma dose in tissues called $D_\gamma$.

Photon-equivalent dose $H_{total}$ (Gy) is the photon equivalent dose of BNCT dose. It was computed by multiplying each absorbed dose component by the relative biological effectiveness (RBE) and compound biological effectiveness (CBE) factors listed in Table 2 (Ishiyama 2014). It was calculated as follows:

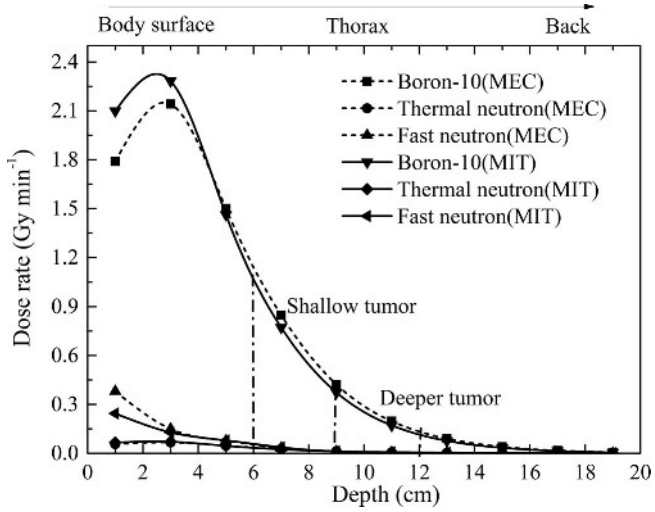


**Fig. 3.** The depth-dose distributions along the central axis of phantom for the MEC and the MIT sources, and the depths for the shallow tumor and the deeper tumor were marked with black dotted line with a 65/18 ppm $^{10}$B concentration in tumor/skin.

**Table 2.** RBE and CF factors (radiation weighting factor wi) used to convert the absorbed dose (Gy) into photon-equivalent dose (Gy).

| BNCT dose component | Normal tissues | Tumor | Skin |
|---|---|---|---|
| $^{10}$B(n, alpha)$^{7}$Li | 1.4 | 3.8 | 2.5 |
| Thermal neutron | 3.2 | 3.2 | 3.2 |
| Fast neutron | 3.2 | 3.2 | 3.2 |
| Photon | 1 | 1 | 1 |

$$H_{total} = \omega_B \times D_B + \omega_{th} \times D_{th} + \omega_f \times D_f + D_\gamma \quad (1)$$

where $\omega_i$ is the radiation weighting factor of dose components ($D_B$, $D_{th}$, $D_f$, and $D_\gamma$) in a particular tissue (Table 2), which is used to convert physical dose (Gy) into photon-equivalent doses (Gy).

## MONTE CARLO CONFIGURATIONS

The general purpose Monte Carlo particle transport code MCNP5 was used to perform the dose calculations in this study. The universe/lattice card, which is a way to simplify the geometry input of repeated structures in MCNP5, was employed in the construction of the human voxel phantom. Each combination of neutron source and $^{10}$B distribution was modeled separately to calculate the dose values. The spherical sources for thermal neutrons were defined by the SDEF card, and different concentrations of $^{10}$B were add in Material Cards of tumor and OARs.

The doses in the tumor and organs at risk were calculated using MCNP5 tally F4 combined DE/DF cards. For the dose conversion, point wise KERMA factors and energy mass absorption coefficients from ICRU 46 were directly input with DE and DF cards. Tally FM4 card was adopted to convert the normalized dose (Gy $s^{-1}$) to photon-equivalent dose (Gy $min^{-1}$). The number of simulated source particles was set to $1 \times 10^9$ in all simulations to make the statistical uncertainty below 2% for the dose results in all the organs of interest.

### Treatment assessment

The doses to OARs including skin and thoracic tissues (right healthy lung, esophagus, heart, liver, breast, and trachea) are relatively higher than any other tissues and organs; thus, they were selected to characterize dose distribution and estimate the efficacy of BNCT treatment according to their maximum dose, minimum dose, average dose and treatment time. In addition, to compare the uniformity of dose in different situations, dose volume curves (DVCs) were depicted.

The minimum dose of GTV should be at least 60 Gy (Suzuki et al. 2012). In addition, the homogeneity index (HI) (Sutlief 2015) of the tumor is defined as:

$$HI = (H_{1\%} - H_{99\%})/H_{50\%} \quad (2)$$

where $H_{a\%}$ is the photon-equivalent dose ($H_{total}$) that is received by a percentage of the structure. A smaller HI value indicates a better dose uniformity. When the dose delivered to the tumor is uniform, the HI is 0.

The dose to OARs should meet the following two limitations according to the National Comprehensive Cancer Network (NCCN) (Ettinger et al. 2013). First, more than 1,000 $cm^3$ of healthy lung should receive less than 7 Gy to prevent pneumonia. Secondly, the maximum dose to heart, spinal cord, skin, esophagus, trachea and bronchi, ribs, and breast should be less than 22 Gy, 14 Gy, 26.0 Gy, 15.4 Gy, 20.2 Gy, 30 Gy, and 50 Gy, respectively.

## RESULTS AND DISCUSSION

### Case 1: Shallow tumor

**Tumor and OARs dose.** When a shallow tumor (distance from the body surface of 6 cm depth) was treated with the MEC and the MIT sources, considering 65 ppm and 18 ppm of $^{10}$B concentration in tumor and skin (65/18 ppm in tumor/skin), the dose to OARs met the NCCN dose limitation (Table 3). The dose to skin and breast irradiated by the MIT source were 33.3% and 18.2% lower than dose induced by the MEC, while the other OARs' dose induced by the MEC were similar to that induced by the MIT source (Fig. 4a).

Compared with the MIT neutron source, the dose rates to the tumor and OARs are higher and the proportion of fast

**Table 3.** The maximum dose to OARs irradiated with the MEC and the MIT sources when the boron concentration in the tumor is 65/18 ppm.

| | Maximum dose (Gy) | | | Differences (%) | |
|---|---|---|---|---|---|
| Healthy tissues/organs | MEC | MIT | Limited dose (Gy) | MEC | MIT |
| Breast | 22 | 18 | 50 | –56% | –64% |
| Heart | 8.3 | 8.4 | 22 | –61.8% | –61.8% |
| Esophagus | 3.0 | 2.8 | 20.2 | –85.1% | –86.1% |
| Trachea | 3.7 | 3.5 | 20.2 | –81.6% | –82.7% |
| Skin | 24 | 16 | 26 | –7.6% | –38.5% |
| Rib | 8.2 | 8.7 | 30 | –72.6% | –71.0% |
| Spinal cord | 1.6 | 1.7 | 14 | –88.5% | –87.5% |
| Cartilage | 29.4 | 26.75 | — | — | — |

neutron dose rates is larger when irradiated with the MEC neutron source. The treatment time (the time required to deliver the prescribed dose to the tumor) is shorter.

Using these two neutron sources, the main ingredient of dose to skin are boron dose and fast neutron dose, and the proportion of fast neutron dose to skin is the largest (Fig. 4b). Besides, the fast neutron dose to skin induced by the MEC is larger than that induced by the MIT source.

The dose to the healthy lung was evaluated to assess physiological impact on the lung. The maximum doses to the right healthy lung were 14 Gy and 12 Gy when irradiated by the MEC and the MIT sources. The maximum dose to the left lung was 10 Gy (Fig. 5) for both sources. In this paper, the volume of the lung is 3,177 $cm^3$, only 14.8% of the volume (331.95 $cm^3$) of the right healthy lung received more than 7 Gy, and 1.5 % of the volume (23.16 $cm^3$) of the left lung received more than 7 Gy. Thus, only 355.11 $cm^3$ of the volume of the lung received more than 7 Gy, namely 2,821.89 $cm^3$ of the volume of the lung received less than

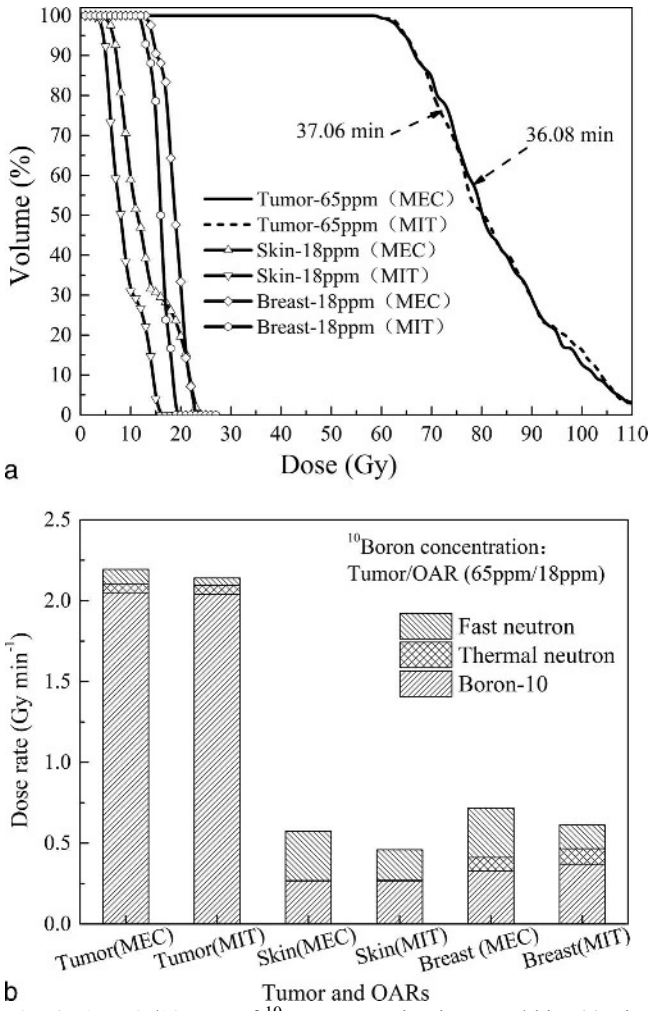


**Fig. 4.** At a 65/18 ppm of $^{10}B$ concentration in tumor/skin: (a) The dose to tumor, skin and breast, and (b) the absorbed-dose rate components to tumor and OARs irradiated with the MEC and the MIT sources.

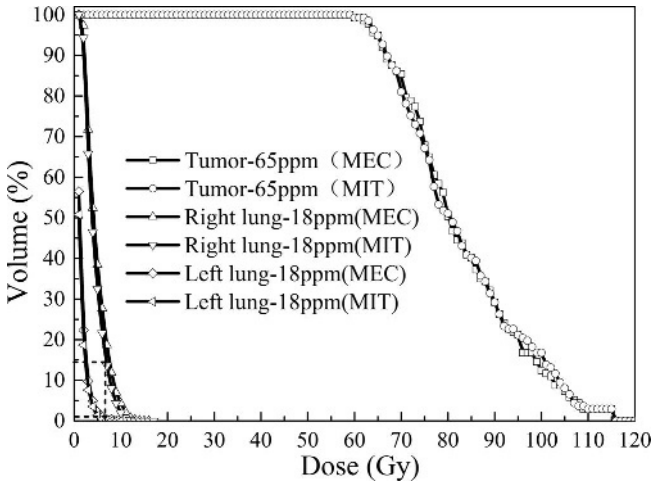


**Fig. 5.** The dose to tumor, left lung and right healthy lung irradiated by the MEC and the MIT sources with a 65/18 ppm ration of $^{10}B$ concentration in tumor/skin.

7 Gy. It fully achieved the requirement of NCCN guidelines of "more than 1,000 $cm^3$ of healthy lung should receive less than 7 Gy to prevent pneumonia" (Ettinger et al. 2013). Therefore, with a 65/18 ppm ratio of boron concentrations in the tumor/skin, the healthy lung will be safe for BNCT when irradiated with these two neutron sources.

**Boron-10 concentration influence on dose to skin and tumor.** Since the dose rate to skin is the largest dose rate and the skin has the smallest limit of the OARs, if the dose to skin is under the 26 Gy dose limitation, the dose to other healthy organs will not exceed the NCCN dose limitation. Here, the relationship between skin dose and boron concentration was studied to explore conditions of boron concentration for BNCT.

When the shallow tumor was treated, dose rates to the tumor and skin increased with increased boron concentration in the tumor and skin, and treatment times declined. At the same time, the value of HI increased, indicating decreased dose uniformity.

With 30 ppm of boron in the tumor, the treatment time was 68 min when irradiated by the MEC. Under this scenario, to maintain a 26 Gy skin dose limit, the dose rate to skin should be lower than 0.38 Gy $min^{-1}$. Therefore, the boron concentration in skin should be less than 8 ppm (Fig. 6b). Under the above condition, BNCT could be performed when the ratio of boron concentration in tumor to that in skin was higher than 3.75.

With an 18-ppm boron concentration in skin, using the MIT source, the maximum dose rate to the skin was 0.41 Gy $min^{-1}$ (Fig. 6b). In this case, the irradiation time should be less than 63 min to maintain the 26 Gy dose limitation to skin. When the irradiation time is 63 min, the boron concentration in the tumor should reach 37 ppm as shown in Fig. 6a. While the dose rate to skin was 0.51 Gy $min^{-1}$

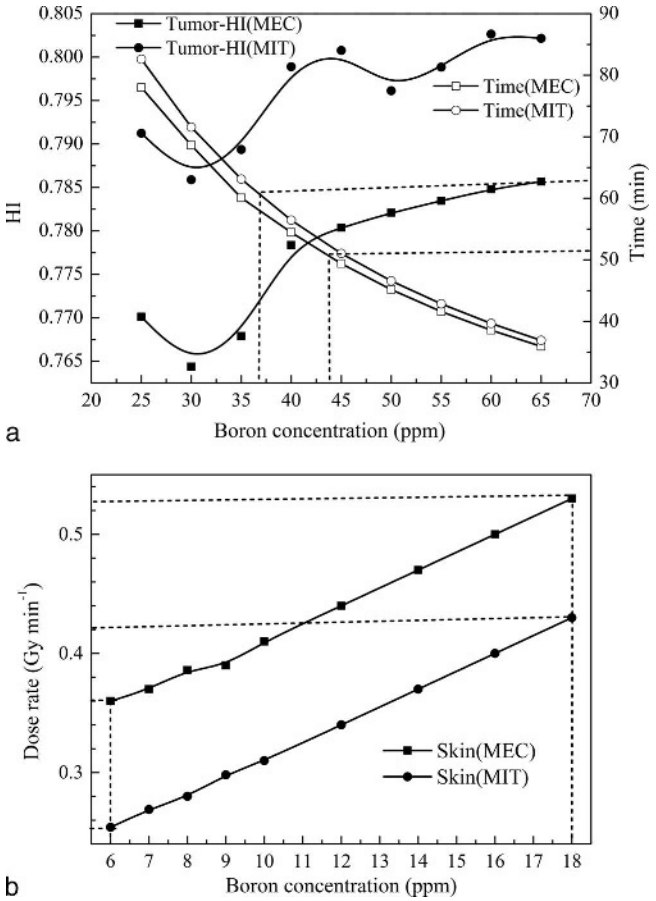


**Fig. 6.** For the shallow tumor: (a) The HI and treatment time changes as a function of the boron concentration in tumor, (b) The maximum dose rates of skin changes with the boron concentration in skin when irradiated by the MIT and the MEC sources.

when irradiated by the MEC (Fig. 6b), the irradiation time would be limited to 50.9 min. Therefore, the boron concentration in the tumor should reach 44 ppm (Fig. 6a).

It can be concluded that the shallow tumor could be treated with BNCT with an appropriate boron concentration with either the MEC or the MIT source. The boron concentration in the tumor treated with the MEC source will be higher than treated with the MIT source.

### Case 2: Deeper tumor

**Tumor and OARs dose.** When a deeper tumor (9 cm from the body surface) was treated with the MIT and the MEC neutron sources, the prescribed dose of 60 Gy was delivered in 81.56 min and 76.25 min, respectively (Fig. 7), which was nearly double the treatment time for the shallow tumor. Here, the $^{10}$B concentration was considered a constant; the boron concentration changes less than 3 ppm (Farias et al. 2014) within 82 min. In addition, compared with the shallow tumor, dose uniformity of the deeper tumor was lower with both neutron sources.

The deeper tumor was treated when the $^{10}$B concentration for tumor/skin was 65/18 ppm. With the MIT source, the skin dose was much less than with the MEC source (Fig. 8) and neither met the NCCN skin dose limitation (Table 4). Moreover, the doses to the most OARs by the MIT source were almost equal to that induced by the MEC source.

When irradiated by the MEC and the MIT sources, the maximum dose to right healthy lung tissue was 25 Gy and 23 Gy, respectively; and the maximum dose to left lung was 16 Gy and 14 Gy (Fig. 9), respectively. Only 40% of the volume of right healthy lung and 4% of the volume of left lung was more than 7 Gy, which fully conformed to the guideline of NCCN. Therefore, treatment would preserve the normal function of lung and will not cause pneumonia when the boron concentration ratio in the tumor/skin is 65/18 ppm.

**Boron-10 concentration influence on dose to skin and tumor.** When the deeper tumor was treated, the dose to skin exceeded the NCCN limit. Therefore, the appropriate $^{10}$B concentration in skin must be determined to reduce the skin dose. From the above analysis, the dose rates reduced as $^{10}$B concentration decreases, so the $^{10}$B concentration in skin was decreased to determine the $^{10}$B concentration that would allow the BNCT to be performed.

At a $^{10}$B concentration in the tumor of 65 ppm, the treatment time was 81.3 min when irradiated with the MIT source. Thus, the dose rate to skin needs to be lower than 0.32 Gy min$^{-1}$ to maintain the 26 Gy dose limitation (Fig. 10a). Therefore, the $^{10}$B concentration in skin should be less than 10.5 ppm, as shown in Fig. 10b. While irradiated with the MEC source, the treatment time was 71.8 min. The $^{10}$B concentration in skin should be less than

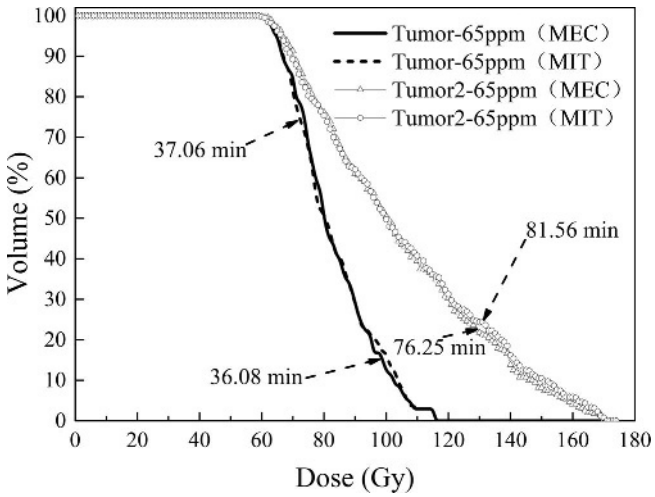


**Fig. 7.** The dose to the shallow and the deeper tumor irradiated by the MEC and the MIT sources with a 65/18 ppm ratio of $^{10}$B concentration in tumor/skin.

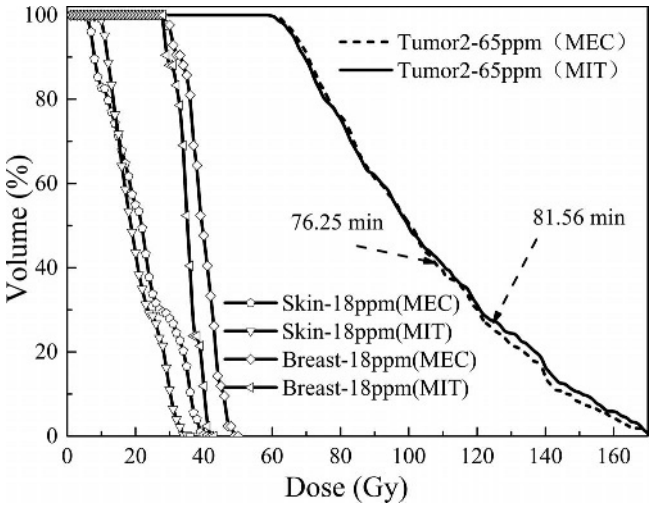


**Fig. 8.** The dose to tumor, skin and breast irradiated by the MEC and the MIT sources with a 65/18 ppm ratio of $^{10}$B concentration in tumor/skin.

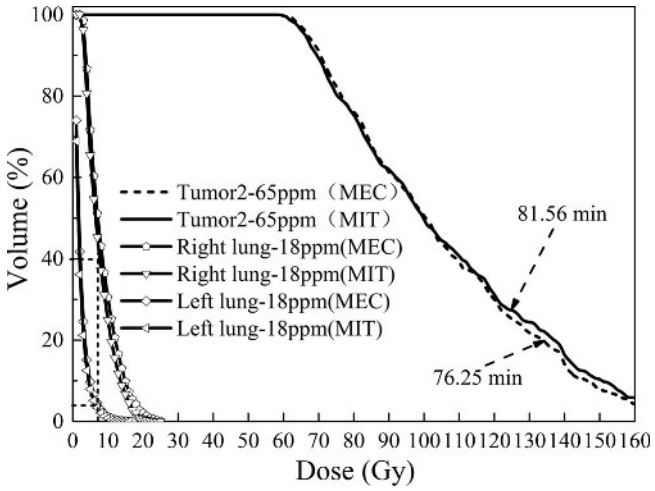


**Fig. 9.** The dose to tumor, left lung and right healthy lung irradiated by the MEC and the MIT sources with a 65/18 ppm ratio of $^{10}$B concentration in tumor/skin.

6 ppm, so that the dose rate to skin is below 0.36 Gy min$^{-1}$ as shown in Fig. 10b.

It can be concluded that the deeper tumor could be treated with BNCT at the appropriate boron concentration condition with either the MEC or the MIT source. The ratios of the boron concentrations in tumors to OARs treated with the MEC source need to be higher than that treated with the MIT source.

## CONCLUSION

Provided that the OARs' dose is within the limitation dose, for the shallow tumor treatment (tumor depth of 6 cm), the MEC source, as compared with the MIT source, is more appropriate for treating and has a shorter treatment time. However, for the deeper tumor treatment (tumor depth of 9 cm), the MIT source is more suitable as the MEC source is more likely to exceed the skin dose limit of 26 Gy. Meanwhile, the deep tumor treatment time was almost double that of the time of the shallow tumor, and the ratio of the boron concentration in tumor to that in OARs is required to be higher than that of the shallow tumor. It could be concluded that a neutron source with more composition of fast neutrons is not necessarily suitable for treating deeper lung tumor directly unless radiation protection measures were taken to reduce the skin dose.

When deep and shallow tumors were treated with the MIT and the MEC sources, attention needs to be paid to the dose to the skin, breast and cartilage as their doses are much higher than any other OARs. As the boron concentration in the tumor and OARs increases, treatment time decreased and dose uniformity of tumors trended downward. Theoretical boron concentration conditions in either the shallow or deep tumor and OARs were obtained, which could help researchers to scale dose to varying assumptions of $^{10}$B concentration and deduce potential dosimetric gains from BNCT when lung tumor was treated with MIT-SPECT or CNEA-MEC.

Admittedly, some factors (for example, beam collimation, beam attenuator and different beam entry angle) could affect the dose distribution in clinical applications. The two case studies presented in the paper were built on ideal irradiations. The dose research in this paper may be of reference value to future projects looking at non-small cell

**Table 4.** The maximum dose to OARs irradiated with the MEC and the MIT sources when the boron concentration in the tumor is 65/18 ppm.

| | Maximum dose (Gy) | | | Differences (%) | |
|---|---|---|---|---|---|
| Healthy tissues/organs | MEC | MIT | Limited dose (Gy) | MEC | MIT |
| Breast | 48 | 41 | 50 | –4.0 % | –18.0 % |
| Heart | 17.5 | 18.48 | 22 | –20.4 % | –16 % |
| Esophagus | 6.3 | 6.4 | 20.2 | –71.3 % | –68.31% |
| Trachea | 7.8 | 7.9 | 20.2 | –61.4 % | –61.8% |
| Skin | 40 | 29 | 26 | +53.8 % | 11.5 % |
| Rib | 17.3 | 19.1 | 30 | –42.3 % | –36.3 % |
| Spinal cord | 3.4 | 3.7 | 14 | –75.7 % | –73.5 % |
| Cartilage | 62 | 58.85 | — | — | — |

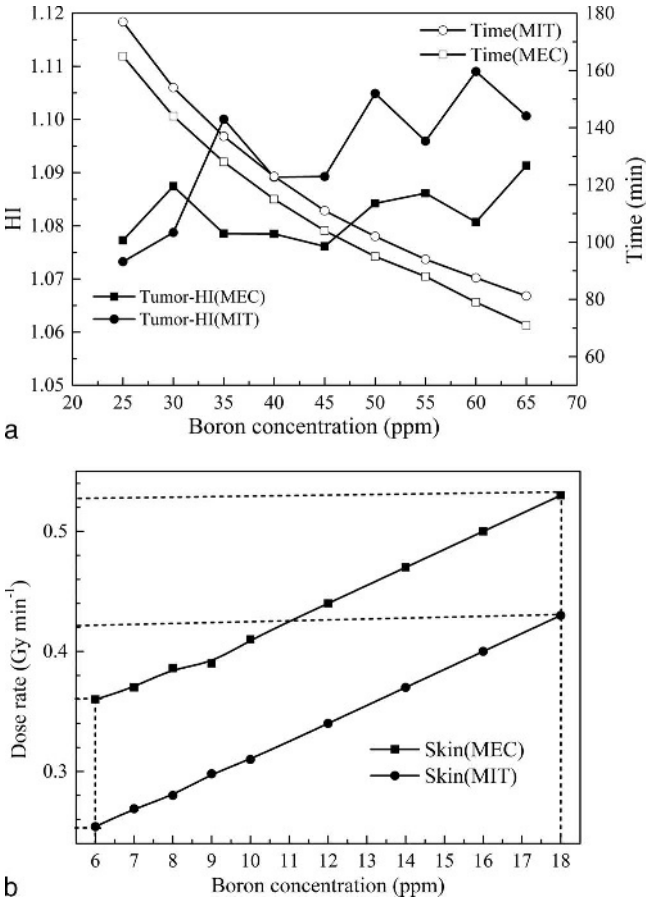


**Fig. 10.** For the deeper tumor: (a) The HI and treatment time changes as a function of the boron concentration in tumor; (b) The maximum dose rates of skin changes with the boron concentration in skin when irradiated by the MIT and the MEC sources.

lung cancer with BNCT. The feasibility of BNCT for this type of cancer has been validated, and the theoretical distribution of $^{10}$B in tumor and organs at risk (especially skin) were obtained to meet the treatable requirement of BNCT, which may provide references for BNCT lung cancer treatment using these two neutron sources.

*Acknowledgment*—This work was supported by the National Natural Science Foundation of China (Grant No. 11475087), the National Science and Technology Support Program (Grant No. 2015BAI34H00), the Foundation of Graduate Innovation Center in NUAA (Grant No. kfjj20150602), and the Priority Academic Program Development of Jiangsu Higher Education Institutions.

## REFERENCES

Coderre JA, Morris GM. The radiation biology of boron neutron capture therapy. Radiat Res 151:1–18; 1999. DOI 10.2307/3579742.

Capoulat ME, Minsky DM, Kreiner AJ. Computational assessment of deep-seated tumor treatment capability of the $^{9}$Be (d, n) $^{10}$B reaction for accelerator-based Boron Neutron Capture Therapy (AB-BNCT). Phys Med 30:133–146; 2014. DOI 10.1016/j.ejmp.2013.07.001.

Ettinger DS, Akerley W, Borghaei H, Chang AC, Cheney RT, Chirieac LR. None small cell lung cancer. Version 2. Journal of the National Comprehensive Cancer Network Jnccn 11:645–653; 2013.

Farias RO, Bortolussi S, Menendez PR, Gonzalez SJ. Exploring Boron Neutron Capture Therapy for non-small cell lung cancer. Phys Medica 30:888–897; 2014. DOI 10.1016/j.ejmp.2014.07.342.

Guitton TG, Kinaci A, Ring D. Diagnostic accuracy of 2- and 3-dimensional computed tomography and solid modeling of coronoid fractures. J Shoulder Elbow Surg 22:782–786; 2013. DOI ***http://dx.doi.org/10.1016/j.jse.2013.02.009***.

Geng CR, Tang XB, Hou XX, Shu DY, Chen D. Development of Chinese hybrid radiation adult phantoms and their application to external dosimetry. Sci China Technol Sc 57:713–719; 2014. DOI 10.1007/s11431-014-5480-x.

International Commission on Radiation Units and Measurements. Photon, electron, proton and neutron interaction data for body tissues. Bethesda, MD: ICRU; Report 46; 1992.

International Commission on Radiological Protection. Basic anatomical and physiological data for use in radiological protection reference values. Oxford: Pergamon Press; ICRP Publication 89, Ann ICRP 32; 2002.

Ishiyama S. Deterministic Parsing Model of the Compound Biological Effectiveness (CBE) Factor for Intracellular $^{10}$Boron Distribution in Boron Neutron Capture Therapy. Journal of Cancer Therapy 5 (14): 1388; 2014. DOI 10.4236/jct.2014.514140.

Koivunoro H, Seppala T, Uusi-Simola J, Merimaa K, Kotiluoto P, Seren T, Kortesniemi M, Auterinen I, Savolainen S. Validation of dose planning calculations for boron neutron capture therapy using cylindrical and anthropomorphic phantoms. Phys Med Biol 55:3515; 2010. DOI 10.1088/0031-9155/55/12/016.

Krstic D, Markovic VM, Jovanovic Z, Milenkovic B, Nikezic D, Atanackovic J. Monte Carlo calculations of lung dose in ORNL phantom for boron neutron capture therapy. Radiat Prot Dosim 161:269–273; 2014. DOI 10.1093/rpd/nct365.

Matsumoto T. Monte Carlo simulation of depth-dose distribution in several organic models for boron neutron capture therapy. Nucl Instrum Meth A 580:552–557; 2007. DOI 10.1016/j.nima.2007.05.233.

Mirzaei D, Miri-Hakimabad H, Rafat-Motavalli L. Depth dose evaluation for prostate cancer treatment using boron neutron capture therapy. J Radiational Nucl Ch 302:1095–1101; 2014. DOI 10.1007/s10967-014-3397-2.

Ryynanen PM, Kortesniemi M, Coderre JA, Diaz AZ, Hiismaki P, Savolainen SE. Models for estimation of the $^{10}$B concentration after BPA-fructose complex infusion in patients during epithermal neutron irradiation in BNCT International. Int J Radiat Oncol 48:1145–1154; 2000. DOI 10.1016/S0360-3016(00)00766-5.

Riley KJ, Binns PJ, Harling OK, Albritton JR, Kiger WS III, Rezaei A, Skold K, Seppala T, Savolainen S, Auterinen I, Marek M, Viererbl L, Nievaart VA, Moss RL. An international dosimetry exchange for BNCT part II: computational dosimetry normalizations. Med Phys 35:5419–5425; 2008. DOI 10.1118/1.3005480.

Sakurai Y, Ono K. Improvement of dose distribution by central beam shielding in boron neutron capture therapy. Phys Med Biol 52:7409; 2007. DOI 10.1088/0031-9155/52/24/014.

Suzuki M, Suzuki O, Sakurai Y, Tanaka H, Kondo N, Kinashi Y, Masunaga S, Maruhashi A, Ono K. Reirradiation for locally recurrent lung cancer in the chest wall with boron neutron capture therapy (BNCT). Internat Cancer Conf J 1:235–238; 2012. DOI 10.1007/s13691-012-0048-8.

Sutlief SG. Protection and measurement in radiation therapy. Health Phys 108:224–241; 2015. DOI 10.1097/HP.0000000000000241.